京都大学医学部保健学科紀要
健康科学　第4巻　2007

原　著

Dissociation of Stimulus-Induced Responses in Regional Cerebral Blood Flow and Blood Volume in the Visual Cortex of Humans

Akitoshi SEIYAMA*,**,***

Abstract: To elucidate hemodynamic response in the human visual cortex during visual stimulation, changes in regional cerebral blood flow (rCBF) and cerebral blood volume (rCBV) were investigated using blood oxygenation-level dependent (BOLD) and flow sensitive alternating inversion recovery (FAIR) functional magnetic resonance imaging (BOLD- and FAIR-fMRI) and 16-channel near-infrared optical imaging (NIOI) techniques. A white and black annular checkerboard (visual angle: 1.2 to 5.8 degrees) focused on perimacular annulus stimulation of the retina, whose temporal frequencies were 0.5, 1.4, 4.7 and 14 Hz with a central fixation point and gray background, was used as the visual stimulus for perimacular annulus. The stimulus-induced activation area obtained with NIOI corresponded to the one measured with BOLD-fMRI. Nevertheless, a dissociation of stimulus-induced responses between the BOLD-fMRI signal and hemoglobin (Hb) parameters obtained with NIOI was found; i.e., changes in BOLD-fMRI signal showed a maximal increase at a temporal frequency of 1.4–4.7 Hz, while increases in oxygenated (oxy-Hb) and total hemoglobin (total-Hb) concentrations showed a minimum around the same frequency, and deoxygenated hemoglobin (deoxy-Hb) showed a slight but significant decrease. This dissociation of stimulus-induced responses of the BOLD-fMRI signal and Hb parameters could be simulated as a function of concentration changes in oxy-Hb, deoxy-Hb, and total-Hb. The temporal frequency dependence of changes in rCBF, estimated from FAIR signal and from the time-course change in total-Hb, was similar to that of the BOLD-fMRI signal change. The present results indicated that stimulus-induced responses of rCBF were dissociated from those of rCBV in the visual cortex of humans during perimacular stimulation at temporal frequency around 1.4–4.7 Hz.

Key words: Near-infrared optical imaging, Functional magnetic resonance imaging, Temporal frequency, Reversal checkerboard, Hemoglobin parameter, Blood oxygenation-level dependent signal

INTRODUCTION

Many of the recent advances in human brain function research have been due to non-invasive functional neuroimaging techniques, especially functional magnetic resonance imaging (fMRI)[1-3]. The application of fMRI to clinical medicine has also rapidly expanded because the technique enables the presurgical determination of pathological changes in neuronal functions and the accurate planning of surgical approaches for brain surgery[4]. On the other hand, during the last decade, another functional neuroimaging technique, near-infrared optical imaging (NIOI), has been developed for monitoring changes in human subjects' hemodynamics[5-7] and neuronal activity[8,9]. Both fMRI and NIOI reflect changes in hemodynamics accompanying changes in local brain activity (i.e., neurovascular coupling).

Stimulus-induced activation of the visual cortex has been extensively studied using electrophysiological techniques[10], positron emission tomography (PET)[11,12], and fMRI[13,14]. Although there was a slight deviation in their results depending on the experimental protocols, the primary visual cortex was maximally activated at a certain temporal frequency, i.e., electrophysiological[10], and oxygen metabolic[12] responses were maximal at around 4 Hz, whereas hemodynamic responses (i.e.,

* Human Health Sciences, Graduate School of Medicine, Kyoto University
53 Kawahara-chyo, Syogoin, Sakyo-ku, Kyoto 606-8507, Japan
** High Performance Bioimaging Research Facility, Graduate School of Frontier Biosciences, Osaka University
1-3 Yamadaoka, Suita, Osaka 565-0871, Japan
*** CREST, Japan Science and Technology Agency
Kawaguchi, Saitama 332-0012, Japan
受稿日　2007年11月7日
受理日　2008年2月14日

changes in rCBF) were maximal at around 8 Hz[11,13,14]. In the later experiments, subjects were shown rather large size of visual stimuli. Further, it has been empirically shown that the neuronal activation induces an increase in rCBF[15] and that the increase in rCBF accompanies an increase in rCBV[16]. Even though Grubb's relationship between CBF and CBV (CBV = $0.8 \cdot CBF^{0.38}$) was determined for adult rhesus monkeys from whole-head measurements under the condition of carbon dioxide inhalation[16], it has been often used for the analysis of stimulus-induced local changes in CBF and CBV.

Recently, we have developed a system capable of simultaneous measurement of fMRI and NIOI for studying stimulus-induced brain activation in the human visual cortex[17]. While fMRI represents an alteration of the difference in the magnetic susceptibility between tissue and blood, NIOI more directly represents hemodynamic parameters such as deoxy-Hb, oxygenated hemoglobin (oxy-Hb), and total hemoglobin (total-Hb) concentrations. The spatial resolution of fMRI is superior to that of NIOI, whereas the temporal resolution of NIOI is superior to that of fMRI. Thus, the two techniques are complementary, and cooperative measurements using fMRI and NIOI possibly provide a way of making more detailed functional brain mappings.

In the present study, by using fMRI and NIOI I aimed to elucidate whether changes in rCBF and rCBV show similar response during stimulus-induced brain activation. During the visual stimulation focused on perimacular annulus of the retina, I examined a temporal frequency-dependence of hemodynamic responses in the human visual cortex using a white and black annular checkerboard. Thereby, I show a dissociation of the stimulus-induced responses between rCBF and rCBV at temporal frequency around 1.4–4.7 Hz, though the stimulus-induced activation areas obtained with these techniques were about the same. Further, I discuss a physiological interpretation of the dissociation between rCBF and rCBV during neuronal activation.

SUBJECTS AND METHODS

Subjects

Six healthy male subjects (24–43 years old) participated in both the fMRI and NIOI measurements. The Communications Research Laboratory approved the experimental protocols. All subjects had normal or corrected-to-normal vision and provided written informed consent. Simultaneous blood oxygenation level-dependent based-fMRI (BOLD-fMRI) and NIOI measurements were performed on three of the six subjects, and for the other subjects, the BOLD-fMRI and NIOI measurements were conducted separately with the same stimuli within three hours after one of the measurements. In addition, one of the six subjects was also conducted with flow sensitive alternating inversion recovery functional magnetic resonance imaging (FAIR-fMRI) and BOLD-fMRI.

Visual stimuli

A white and black annular checkerboard, with a central fixation point and gray background, was used as the visual stimulus (perimacular annulus, 1.2 to 5.8 degrees; angle of each wedge, 10 degrees; number of ring-layers, 5; temporal frequency, 0.5, 1.4, 4.7, and 14 Hz) (Fig. 1). With the checkerboard, visual stimulation longer than 16 s gave a good correlation in hemodynemic responses between NIOI and fMRI signals (e.g., r = 0.87, 0.85, 0.91, and 0.95 for 4, 8, 16, and 32 s of stimulus duration, respectively)[18]. The time sequences of experiments consisted of [control (14 s) + stimulation (28 s) + control (14 s)] for BOLD-fMRI and NIOI measurements, and [control (12 s) + stimulation (32 s) + control (12 s)] for additional BOLD- and FAIR-fMRI measurements. Each of four different reversal frequencies was used four times in pseudo-

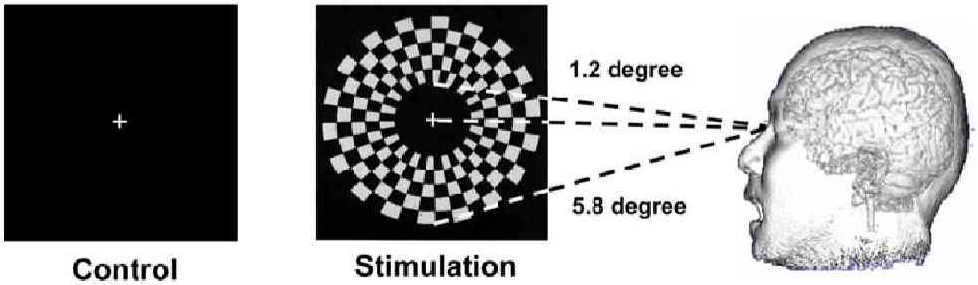

Fig. 1 Illustration of visual stimuli. A white and black annular checkerboard, with a central fixation point and gray background, was used as the visual stimulus (perimacular annulus, 1.2 to 5.8 degrees; angle of each wedge, 10 degrees; number of ring-layers, 5; temporal frequency, 0.5, 1.4, 4.7, and 14 Hz). Other details are shown in the text.

random order for about 15 min. During the control and stimulation periods, the subjects were required to fixate on the fixation cross placed on the center of the checkerboard.

MRI acquisition and analysis

A 1.5-T MRI scanner (Magnetom Vision; Siemens, Germany) was used for obtaining functional images with an echo-planar imaging (EPI) sequences. Flow sensitive alternating inversion recovery (FAIR) functional magnetic resonance images (FAIR-fMRI) were obtained with repetition time (TR)=2,000 ms, echo time (TE)=15.7 ms, flip angle (FA)=90°, field of view (FoV)=256×256 mm^2, matrix size=64×64, and inversion time (TI)=1,400 ms. A 10-mm oblique imaging slice and an inversion slab (thickness, 20 mm) were selected along the calcarine fissure to cover the primary visual cortex. FAIR images were obtained from subtraction of non-slice-selective inversion recovery (IR) images from slice-selective IR images. Blood oxygen level-dependent (BOLD) based functional images were obtained with TR=4,000 ms, TE=55.24 ms, FA=90°, FoV=256×256 mm^2, and matrix size=64×64. Thirty-two axial slices were obtained (thickness of slice, 4 mm; slice gap, 0 mm; pixel size, 4×4 mm^2). Number of scans was 236, where the first five images were discarded to eliminate spin saturation effects. Anatomical images of the brain were obtained with a T_1-weighted sequence (TR, 9.7 ms; TE, 4 ms; FA, 12°; FoV, 256×256 mm; matrix size, 256×256). Areas of significant activation were processed using SPM99 (http:// www.fil.ion.ucl.ac.uk), determined according to the statistical threshold at $p<0.05$ (voxel level, corrected for multiple comparisons with in the entire search volume), and were displayed in rendered T_1 images of each individual subject. To compare the MR signals with the optical signals (pixel size: ca. 20×20 mm^2, see below), the time courses of the MR signals from the region of interest were obtained using AVS/Express version 3.2 (Advanced Visual Systems Inc., USA) for BOLD-fMRI signals and a laboratory product MR Interactive Browser (FMIB) for FAIR-fMRI signals. The MR signals corresponding to the optical voxel estimated by NIOI was identified with oil markers (see arrows in Fig. 2 (C) and its legend). After the group of 5×5×5 MRI voxels was selected to cover the optical voxel, MR signals from the scalp and from the cortex were separated as follows. The MR signal from the scalp was that from the first and second layers of the fMRI voxels from the scalp surface (i.e., averaged signal of 5×5×2 voxels (20×20×8 mm^3)). The MR signal from the cortex was obtained by averaging the MR signals over the fifth (deepest) layer (5×5×1 voxels, 20×20×4 mm^3).

Optical measurement and analysis

Details of optical measurement and analysis are also described elsewhere[19]. In brief, a 16-channel NIOI system, OPTIM_A, was used to obtain functional optical images and changes in hemoglobin (Hb) species concentrations from resting conditions (i.e., Δ[oxy-Hb], Δ[deoxy-Hb], and Δ[total-Hb] (=Δ[oxy-Hb]+Δ[deoxy-Hb]). Combinations of 16 nearest-neighbor pairs of input and output fibers were used to obtain a topographical image covering a 76×76 mm^2 area in the occipital region of the head. Data were acquired at temporal resolution of 400 ms. The image had an NIOI pixel size of 20×20 mm^2 obtained at a source-detector distance of 27 mm (see Fig. 2 (A)). Our NIOI system, OPTIM_A, can also be used in spatially resolved spectroscopy (SRS). In the present study, the light reflected from the brain was collected by light guide detectors placed at two different locations, with the proximal one at 20 mm and the distal one at 40 mm from the incident light guide, to obtain the absolute basal values of the Hb species concentration ($[oxy\text{-}Hb]_{rest}$, $[deoxy\text{-}Hb]_{rest}$, and $[total\text{-}Hb]_{rest}$) and oxygen saturation in the blood (Sa_{rest}) of the brain in the resting state before the experiment.

Reconstruction of BOLD signal using NIOI data was performed using the following equation[19]:

$$S_{stim} = S_{rest} \cdot [1 + TE \cdot \alpha^* \cdot \{\Delta Sa/(1-Sa_{rest}) - \beta^* \cdot \Delta[total\text{-}Hb]/[total\text{-}Hb]_{rest}\}], \quad (1)$$

If the source of the signal reflects regions containing venules or larger veins, β^* will be 1 (the Vein model), and if the source of the signal reflects regions containing capillaries, β^* will be 0.5 (the Capillary model). In the present study, values of α^* for the Vein and Capillary models were 16.11 s^{-1} and 32.22 s^{-1}, respectively, which were experimentally determined by measuring MR signal at resting state using various values of TEs (33.24, 45.24, 55.24, and 65.24 ms).

Calculation of ΔrCBF and ΔrCBV from NIOI data

The Fick principle depends upon the fact that the rate of accumulation of a tracer substance in an organ equals the difference between its rate of arrival and its rate of departure from that organ. If the rate of accumulation of a tracer is measured at a time less than the minimum transit time of that tracer throughout the organ, the departure of the tracer is considered zero and the flow

rate can be estimated from the accumulated amount of tracer.

In the present case, ⊿[total-Hb] was used as an intravascular tracer, so we assumed that the increase in [total-Hb] was brought about by a sudden increase in ⊿rCBF caused by neuronal activation, and that the outflow was unchanged until a certain short time period. Here, the time was taken to be 2 sec after onset of increase in ⊿[total-Hb], because mean transit time of cerebral blood circulation measured by a near-infrared spectroscopy is ca. 6 sec[20]. The index of ⊿rCBV was obtained by averaging ⊿[total-Hb] during stimulation. Then, each parameter was converted into the units of ml/min/100 g tissue for ⊿rCBF and of ml/100 g tissue for ⊿rCBV as follows. $\Delta rCBV = \{k/(R \cdot [Hb]_A)\} \cdot \Delta[\text{total-Hb}]$, where $[Hb]_A$ is arterial total Hb concentration (assumed 15 g/dl$_{blood}$) and k ($= 10^{-6} \cdot MW_{Hb}/(10 \cdot Dn)$) is a constant reflecting the molecular weight of Hb (MW_{Hb}, 64,500 (Hb base)) and tissue density (Dn, 1.05 g/ml)[21], and R is cerebral-to-arterial hematocrit ratio (0.69)[22]. $\Delta rCBF = (k/[Hb]_A) \cdot (d\Delta[\text{total-Hb}]/dt)$. The unit of [total-Hb] (or ⊿[total-Hb]) is mmoles per liter of tissue.

Statistics

Data are expressed as the mean ± standard deviation (SD). A one-way analysis of variance (ANOVA) with repeated measurement in combination with Bonferoni multiple comparisons test was used, and values of $p < 0.05$ were considered statistically significant.

RESULTS

Fig. 2 shows a typical example of the stimulus-

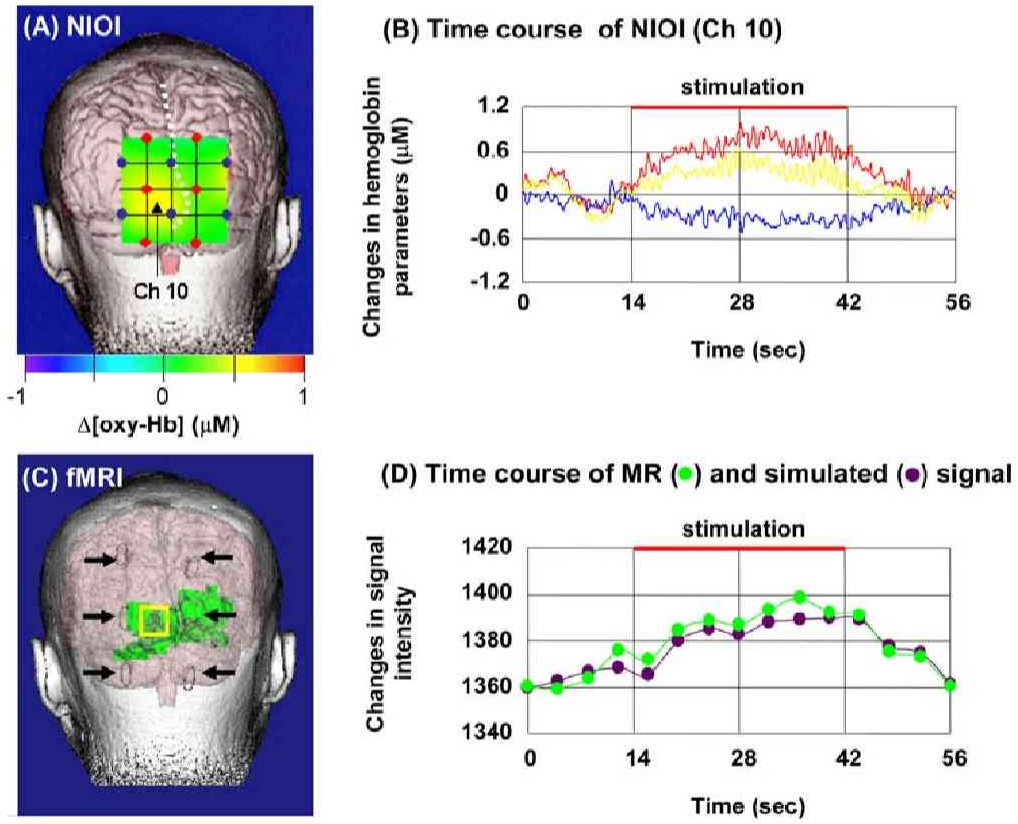

Fig. 2 A typical example of stimulus-induced activation in the occipital cortex. (A) The map of ⊿[oxy-Hb], obtained with NIOI (OPTIM A), was superposed on the T_1-MRI structure, where the source (red circle) and detector (blue circle) positions are superposed. The white broken line denotes the position of the longitudinal fissure. (B) Time course of changes in concentrations of Hb species (⊿[oxy-Hb], red line; ⊿[deoxy-Hb], blue line; ⊿[total-Hb], yellow line) in the activation area (Ch 10), whose position is shown in (A) with an arrow. (C) Stimulus-induced activation area obtained with BOLD-fMRI analyzed using SPM 99 (thresholded at voxel-level $p < 0.05$). Arrows indicate positions of oil markers attached to the scalp of the subjects to register the map of BOLD-fMRI and NIOI. (D) Time courses of changes in MR (green) and simulated (dark purple) signals. The change in the MR signal in the primary visual cortex was obtained from the square area in (C), which corresponds to the NIOI pixel showing maximal increase in ⊿[oxy-Hb] (Ch 10 in A). The change in the simulated signal was obtained using the Vein model in Eq. 1 and the Hb parameters of Ch 10 shown in (B). The initial values of S_{rest} and $T_e \cdot R^*_{2rest}$ as measured before task presentation were 1,360 and 0.89, respectively, and Sarest and $[\text{total-Hb}]_{rest}$ were 0.702 and 51.4 μM, respectively. The maps and the time courses show the average of four measurements at a stimulus frequency of 1.4 Hz.

induced activation in the occipital cortex obtained with NIOI (Figs. 2A and 2B) and fMRI (Figs. 2C and 2D). During visual stimulation, each of our subjects showed significant changes in the signal intensities of fMRI (and NIOI) in the occipital lobe along the calcarine fissure, anatomically defined as the striate cortex (primary visual area) and part of the extrastriate cortex. The activation area measured with NIOI (Δ[oxy-Hb]) (Fig. 2A) corresponded to the one measured with fMRI (Fig. 2C), in which the primary visual area of the left hemisphere of this subject was included in channel 10 (Ch 10) in Fig. 2A. Thus, we compared the temporal pattern of NIOI (Fig. 2B) and fMRI (Fig. 2D) in the primary visual area of the left hemisphere. The temporal patterns of changes in Hb parameters (Δ[oxy-Hb] or Δ[total-Hb]) were similar to that of the MR signal. Furthermore, the simulated MR signal agreed well with the actual one. Similar results were obtained for all subjects, and, thus, the NIOI pixel showing maximal increase in Δ[oxy-Hb] for individual subjects was selected as a region of interest for comparison of NIOI and fMRI signals, and it was the same for all frequency and corresponded to the primary visual cortex of each subject. Fig. 3 shows a typical example of maps of hemodynamic responses in the visual cortex at temporal frequencies ranging from 0.5 to 14 Hz. The statistical parametric map of fMRI showed a similar area of activation for all the frequencies (top row), but the change in MR intensity in the primary visual area was larger at the temporal frequency of 4.7 Hz (cf. rhombic symbols of subject 1 in Fig. 4), while the changes in the concentrations of Hb species (especially Δ[oxy-Hb] and Δ[total-Hb]) were larger at 0.5 or 14 Hz (cf. square and triangle symbols of subject 1 in Fig. 4) than at other frequencies. The changes in Hb parameters and the MR signal from a channel including the primary visual area of individual subjects are shown in Fig. 4. The BOLD-fMRI signals' maximums were at a temporal frequency of 1.4 or 4.7 Hz in all subjects, whereas increases in Δ[oxy-Hb] and Δ[total-Hb] reached minimums at these stimulus frequencies, and decrease in Δ[deoxy-Hb] reached maximum.

Fig. 5 compares the simulated BOLD signals using Eq. 1 with the BOLD-fMRI signals itself. The absolute values of the hemodynamic parameters in the occipital cortex in the resting state are summarized in Table 1, and were used for the simulation. The simulation using

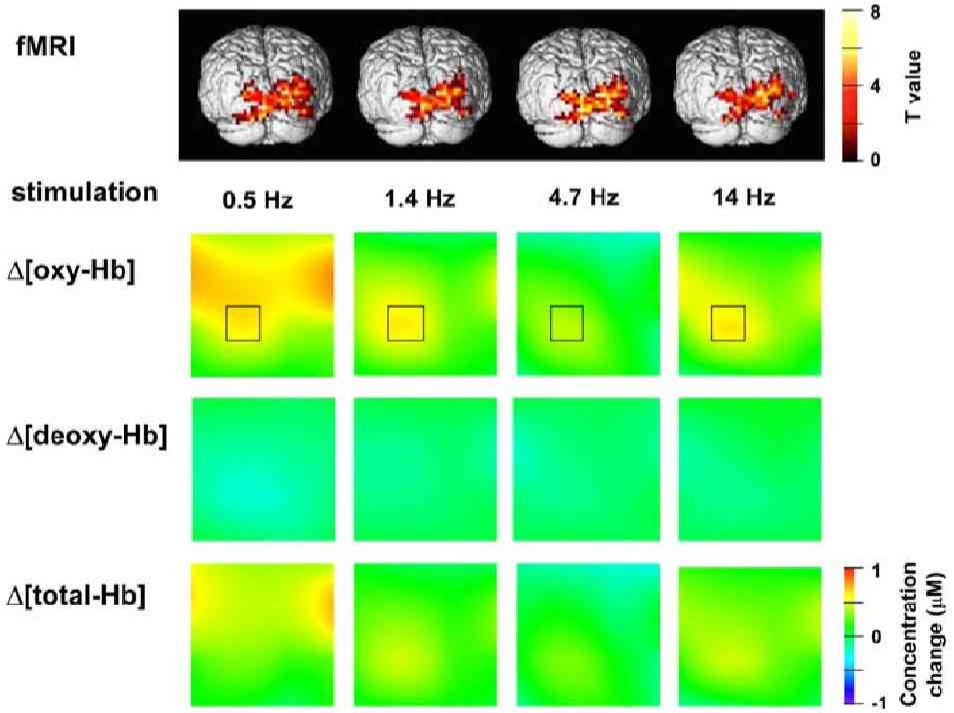

Fig. 3 A typical example of stimulus-induced responses of the occipital cortex at four stimulus frequencies. Top row, maps of BOLD-fMRI ($P<0.05$) ; 2nd row, maps of Δ[oxy-Hb] ; 3rd row, maps of Δ[deoxy-Hb] ; Bottom row, maps of Δ[total-Hb]. The maps of the vertical columns correspond to individual temporal frequencies, 0.5, 1.4, 4.7, and 14 Hz. The NIOI pixel which showed maximal increase in Δ[oxy-Hb] is indicated by a black square and selected as a region of interest for comparison of NIOI and fMRI signals, which was the same for all frequency and corresponded to the primary visual cortex. The maps show the average of four measurements with the individual stimulus frequency of the checkerboard, and show averages over time during stimulation. The scale of the Hb parameters' color bar is the same as shown in Fig. 2A.

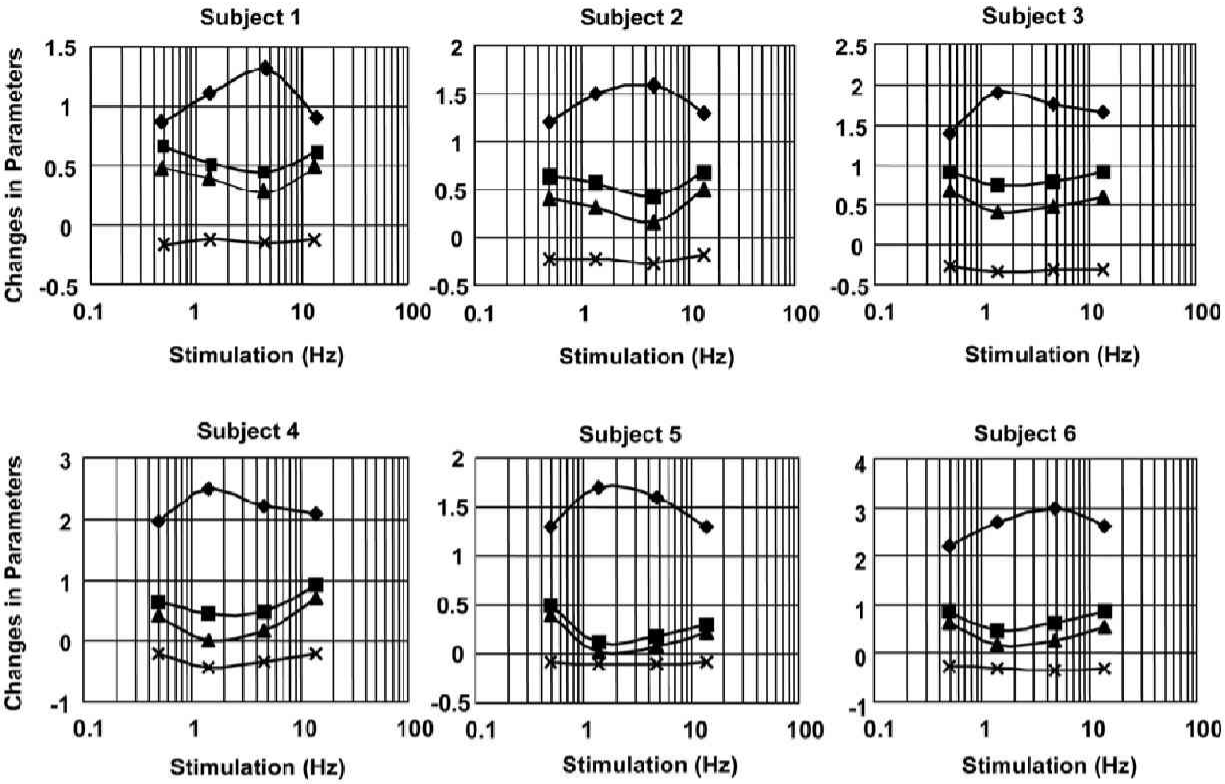

Fig. 4 Temporal frequency dependence of stimulus-induced responses of the occipital cortex of individual subjects. The ROI, corresponding to single channel of NIOI, was selected as shown in Fig. 3. ◆, BOLD-fMRI signal (%) ; ■, Δ[oxy-Hb] (μM) ; ▲, Δ[total-Hb] (μM) ; x, Δ[deoxy-Hb] (μM). The values denote averages over time during stimulation for 4 tasks. Simultaneous measurements of fMRI and NIOI were performed on subject 2, 4 and 6. The averages over 6 subjects and their statistics are shown in Fig. 6A.

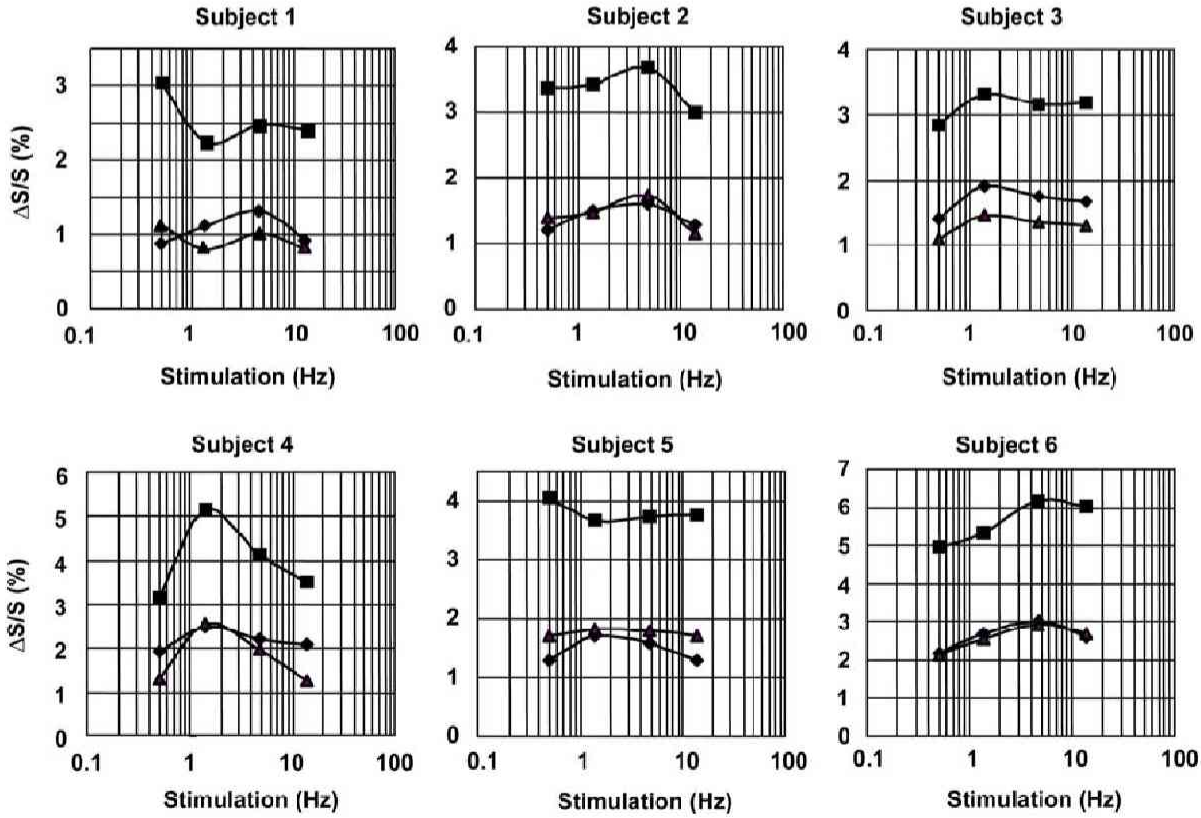

Fig. 5 Simulation of stimulus-induced responses of BOLD-fMRI signal using Hb parameters obtained with NIOI. Data from the channel in which the maximal change in the hemodynamic parameter was observed in individual subjects are shown. The vertical axis, $\Delta S(=S_{stim}-S_{rest})/S$ (%), denotes changes in simulated BOLD signals and measured BOLD-fMRI signals itself. The triangle and square symbols show simulated BOLD signals using the Vein and Capillary model in Eq. 1, respectively. The rhombic symbols indicate the BOLD-fMRI signal.

Table 1 Resting values of Hb parameters in the human occipital cortex.

Parameters Unit	Sa_{rest}	$[oxy\text{-}Hb]_{rest}$ (μM)	$[deoxy\text{-}Hb]_{rest}$ (μM)	$[total\text{-}Hb]_{rest}$ (μM)	CBV_{rest} (ml/100 g tissue)
Subject 1	0.702	36.12	15.33	51.44	3.06
Subject 2	0.776	50.24	14.54	64.78	3.84
Subject 3	0.765	69.24	21.25	90.49	5.37
Subject 4	0.758	48.23	15.40	63.70	3.78
Subject 5	0.729	42.25	15.68	57.93	3.41
Subject 6	0.845	60.60	11.05	71.65	4.25
Mean	0.763	43.59	15.54	66.67	3.95
SD	0.049	22.59	3.28	13.51	0.81

Absolute values of Hb parameters at rest were estimated with the spatially resolved spectroscopy mode of OPTIM_A. The values indicated the average over 10 min in the resting state before experiments.

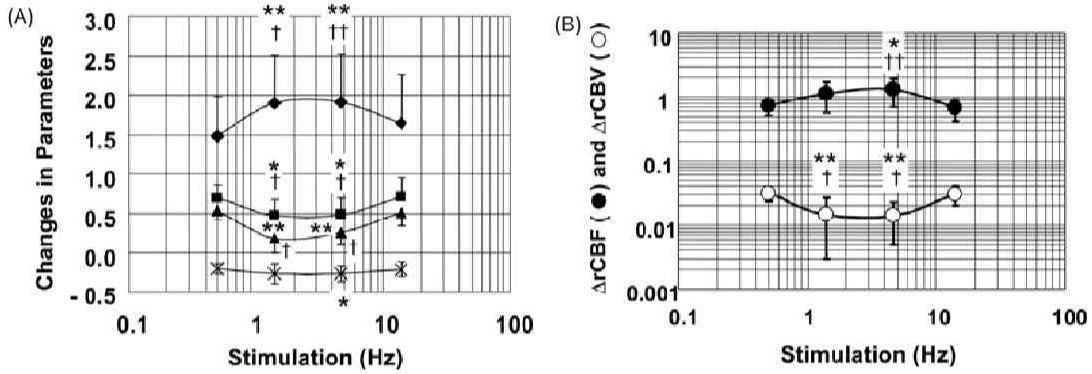

Fig. 6. Hemodynamic responses induced by visual stimulation with a white and black annular checkerboard. (A) Changes in BOLD-fMRI (%) and hemodynamic parameters (μM) obtained from 6 subjects. Data for individual subjects are shown in Fig. 4, and symbols and units of the parameters are the same as those in Fig. 4. (B) Changes in rCBF (ml/min/100 g tissue, closed circle) and rCBV (ml/100 g tissue, open circle) estimated from stimulus-induced changes in [total-Hb] (see Subjects and Methods). The values show the mean±SD from 6 subjects. *, $p<0.05$ vs 0.5 Hz; **, $p<0.01$ vs 0.5 Hz; †, $p<0.05$ vs 14 Hz; ††, $p<0.01$ vs 14 Hz.

the Vein model (triangle symbols) satisfactorily reproduced the stimulus frequency dependence of changes in the BOLD-fMRI signal (rhombic symbols), especially for those of simultaneous measurements (subjects 2, 4 and 6), while the simulation using the Capillary model (square symbols) deviated largely from the BOLD-

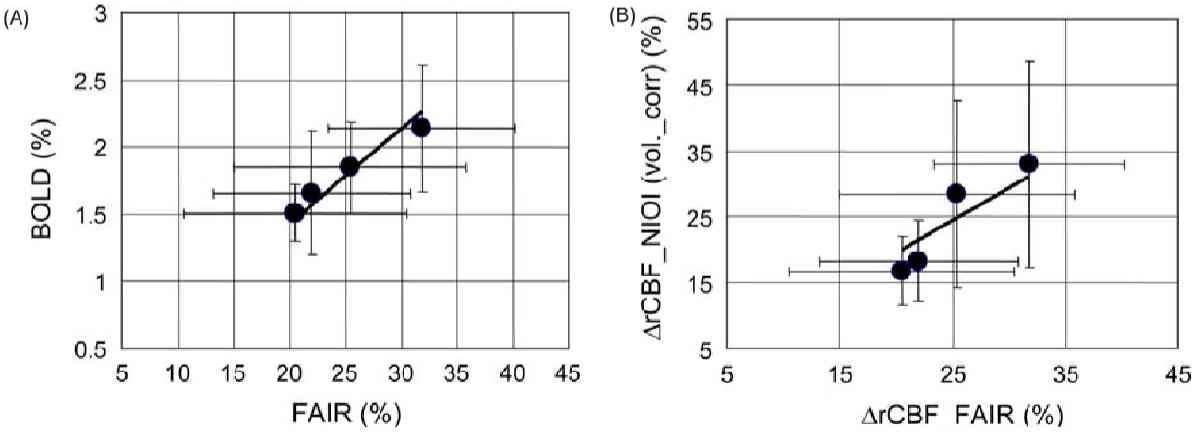

Fig. 7 Stimulus-induced hemodynamic responses measured with BOLD-, FAIR-fMRI, and NIOI. (A) Relationship between BOLD- and FAIR-fMRI signals. Linear regression gave the relation of BOLD (%)=0.0713×FAIR (%) and the correlation coefficient (r) of 0.934. (B) Relationship between changes in rCBF obtained with NIOI (ΔrCBF_NIOI (vol_corr)) and FAIR (DrCBF_FAIR) measurements. Linear regression gave the relation of ΔrCBF_NIOI (vol_corr) (%)=0.983×ΔrCBF_FAIR (%) and r=0.893. For the volume correction of ΔrCBF_NIOI (vol_corr), optically estimated ΔrCBF is multiplied by a factor of 25, which corresponds to the ratio of pixel size of NIOI and FAIR (see Materials and Methods). The values show the mean±SD from 4 tasks. The marks denote 0.5, 14, 1.4 and 4.7 Hz from left to right.

fMRI signal. This result indicates that the BOLD-fMRI signal obtained with the 1.5 T MR system reflects mainly the cortical area containing venules and/or larger veins, but not the capillary bed as predicted. Further, present result agreed with the result that NIRS signal mainly reflected the information from venules and/or larger veins[23].

Fig. 6A shows the averaged values of changes in parameters measured with fMRI and NIOI for the six subjects. The BOLD-fMRI signal showed a maximum at temporal frequencies between 1.4 and 4.7 Hz, whereas Δ[oxy-Hb] and Δ[total-Hb] obtained using NIOI showed a minimum at these frequencies. Decrease in [deoxy-Hb] was small but significant at 4.7 Hz ($p<0.01$ vs 0.5 Hz). To clarify this dissociation of responses between the BOLD-fMRI signal and Hb parameters, stimulus-induced changes in rCBF and rCBV were estimated from the time course of Δ[total-Hb] (Fig. 6B). Changes in the BOLD-fMRI signals well corresponded to changes in estimated rCBF, while changes in [total-Hb] (and [oxy-Hb]) corresponded to the changes in rCBV. More directly to ascertain stimulus-induced changes in rCBF, we performed the FAIR measurement (Fig. 7). Fig. 7 shows that changes in FAIR-fMRI signals well correlated with those of BOLD-fMRI signals (BOLD (%) = 0.07 · FAIR (%), r = 0.934), and with optically estimated changes in rCBF (ΔrCBF_NIOI = 0.983 · ΔrCBF_FAIR, r = 0.893).

DISCUSSION

Effect of temporal frequency on neuronal activation and BOLD signal

The dependence of neuronal activity upon temporal frequency of stimulus is well documented in animals[24,25]. The maximal responses in the visual cortex occurring around 8 Hz could be related to the sensitivity of retinal ganglion cells and their firing rate[24] or to the contrast sensitivity of neurons in Brodmann's areas 17 and 18[25]. As for humans, it has been reported that the electrical response[10] and $rCMRO_2$ response[12] showed a maximum at a temporal frequency around 4 Hz when a checkerboard was used for visual stimulation, while the rCBF response to flash photic stimulation showed a maximum at a temporal frequency around 8 Hz[11,13,14]. Our present results, which were obtained for the stimulation with a reversal white/black checkerboard with a gray background, showed the maximum response of the BOLD-fMRI signal and minimum response of the Hb parameters (oxy-Hb and total-Hb) at temporal frequencies ranging from 1.4 to 4.7 Hz (Figs. 3 and 4). The frequency range at which the maximal BOLD-fMRI response was observed in the present experiments was similar to those of the electrical response[10] and $rCMRO_2$ response[12], where the stimulation was conducted with a checkerboard. However, the maximum hemodynamic response to flash photic stimulation occurred around double this frequency range[11,13,14]. The following two possibilities can be considered to explain the above discrepancies. As one of possibilities, in experiments using checkerboards, the frequency of stimulation is considered to be twice the white-to-white or black-to-black frequency of the checkerboard, if the visual stimulus basically comes from pattern reversal. If so, the frequency of 1.4–4.7 Hz corresponds to 2.8–9.4 pattern reversals/sec (twice the stimulus frequency). Thus, during a visual stimulation with a varying temporal frequency, the BOLD-fMRI signal attains its maximum at the frequency of maximal neuronal activation. Another possible explanation is as follows. It is reported that the size of visual stimulus affects the contrast sensitivity of retina, i.e., as the stimulus area is larger, the retina shows high sensitivity at the higher temporal frequency[26–28]. The checkerboard used in the present study (visual angle is 1.2–5.8 degree) stimulates the perimacular annulus. The retina showed a high contrast sensitivity at lower temporal frequency than 8 Hz in this small visual angle stimulation. Recent reports[29,30], which showed a maximal response at temporal frequency above 10 Hz using wide visual angle stimulation (33–45 degree), may support the latter possibility.

Stimulus-induced changes in rCBF and rCBV

In the previous study, we have shown a temporal analysis of BOLD-fMRI signal using NIOI signals[19], in which the Vein model in Eq. 1 could well express the changes in stimulus-induced change in BOLD-fMRI signals (see also Fig. 2D). The present results show that Eq. 1 (the Vein model) is also satisfactorily useful for the steady state analysis of BOLD-fMRI signals (Fig. 5), since data analyzed were averages of four measurements, and averaged over time during stimulation. The absolute values of the hemodynamic parameters in the resting state in the occipital cortex are summarized in Table 1. Recently, spatially resolved[31–33] or frequency-domain[34] near-infrared spectroscopy has been often used to obtain absolute concentration of cerebral Hb species concentrations and hemoglobin oxygenation. Although these techniques

have been used for measurements on the forehead, our estimated values of Hb species concentrations in the occipital cortex (Table 1) are similar to those reported previously. Values of CBV_{rest} measured using PET are only comparable data reported hitherto. Although there were considerable differences among the individual subjects, optically estimated CBV_{rest} agreed well with those obtained by PET and erythrocyte tracers: 4.2±0.4 ml/100 g brain tissue[35], 4.3±0.41 ml/100 g brain tissue[36], and 4.34±0.5 ml/100 g brain tissue[37]. However, the value of ⊿rCBF estimated from NIOI is 3.2% (ranging from 2.2 to 4.2%) of the basal value, and that of ⊿rCBV is 0.6% (ranging from 0.4 to 0.8%) of the basal value. These changes are about one order smaller than those reported by others using PET (49.6±13.9% for ⊿rCBF[38]; 4.4–16.5% for ⊿rCBV[39]) and fMRI (42.8±15.9% for ⊿rCBF, and 14±5% for ⊿rCBV[40]), although the changes in the concentrations of the Hb species detected in the present experiment using NIOI were similar to those reported by others on visual stimulation in humans[41,42]. To ascertain this discrepancy, we compared the optically estimated ⊿rCBF with those obtained with FAIR-fMRI (Fig. 7B). When the appropriate volume correction was applied between those two techniques (i.e., NIOI vs FAIR-fMRI), ⊿rCBFs obtained with these techniques were almost identical (slope = 0.983) with good correlation (r=0.893), where for the volume correction of ⊿rCBF_NIOI (vol_corr), optically estimated ⊿rCBF is multiplied by a factor of 25, which corresponds to the ratio of pixel size of NIOI and FAIR (see Materials and Methods). Furthermore, FAIR-fMRI signal gave a linear relationship with BOLD-fMRI signal (Fig. 7A) with good correlation (r=0.934), which agreed with the results reported by Kwong et al.[13] and Zhu et al.[43]. The above results indicate that during visual stimulation the BOLD signal reflects ⊿rCBF, while the NIOI signal (⊿[total-Hb]) reflects ⊿rCBV (Fig. 6A vs 6B).

Physiological implications of decoupling between ⊿rCBF and ⊿rCBV

It has been empirically shown that the increase in rCBF accompanies an increase in rCBV[16]. Though Grubb's relationship between CBF and CBV ($CBV = 0.8 \cdot CBF^{0.38}$) was determined for adult rhesus monkeys from whole-head measurements under the condition of carbon dioxide inhalation, it has been often used for the analysis of stimulus-induced local changes in CBF and CBV. In contrast with their result, in the present study, we have shown a dissociation of the stimulus-induced responses between rCBF and rCBV at temporal frequency around 1.4–4.7 Hz, though the stimulus-induced activation areas obtained with these techniques were about the same.

Recently, it was shown that the BOLD signal correlates with neuronal activation reflecting the local field potential response rather than the action potential response[44]. In addition, it has been shown that during neuronal activation in the human visual cortex[38], the regional cerebral metabolic rate of glucose ($rCMR_{glc}$) increases to a similar extent as the rCBF increases; i.e., a close coupling exists between $⊿rCMR_{glc}$ and ⊿rCBF. However, DrCBF is accompanied by a rather smaller $⊿rCMRO_2$ (e.g., ⊿rCBF; $⊿rCMRO_2 = 10$; 1[38]; ⊿rCBF; $⊿rCMRO_2 = 2$: 1[45]), suggesting that the supply of oxygen is not matched precisely with the demand. Several models based on the enzyme-limited[38] or diffusion-limited oxygen-delivery theory[46–48] have been proposed to explain the overcompensation of oxygen inflow. In the context of the enzyme-limited model, Fox et al.[38] postulated that (i) enzyme activity coupled with oxidative phosphorylation of glucose is kept at or near the maximal level (even under resting conditions) to maintain the electrophysiological activity of neurons, and that (ii) the acute energy expenditure accompanying neuronal activation is supported by anaerobic glycolysis. This means that during neuronal activation, the blood flow is regulated by a mechanism other than oxidative metabolism, probably to washout the end product of the anaerobic glycolysis pathway, lactate, and to restore the decreased pH. In the context of the diffusion-limited oxygen delivery model, Buxton[49] postulated that a large increase in rCBF is required to support a smaller increase in oxygen metabolism because the oxygen extraction fraction decreases with increasing rCBF. However, both theories may not fully explain why the supply of oxygen can differ largely from the demand. The explanations are incomplete because the disparity between ⊿rCBF and $⊿rCMRO_2$ during neuronal activation does not appear under all circumstances and in all regions of the brain. For example, Roland et al.[50] reported a strong relationship between ⊿rCBF and $⊿rCMRO_2$ in the prefrontal cortex, frontal eye fields, parietal lobe, and thalamus during mental calculation.

Based on the above findings and discussions, I here propose that the increase in rCBF is not for supplying oxygen but for supplying other substances, i.e., glucose. This implies that the glucose transport by plasma is given priority over the oxygen transport, almost all of

which is carried out by hemoglobin within erythrocytes (i.e., oxy-Hb), because an increase in the metabolic rate of glucose corresponds well to that in CBF[38]. Then, the dissociated responses between ⊿rCBF and ⊿rCBV, which occurs at maximal neural activity and $rCMRO_2$, could serve to prevent the following shortcomings by reducing the oxygen carrier, erythrocytes; 1) excess inflow of oxygen in the focal activated area and 2) increase in the resistive force due to the increased rCBF. Possible mechanisms for this dissociation between rCBF and rCBV responses are as follows: 1) relocation of tissue water to blood compartment at capillary area[51,52], and 2) redistribution of blood flow or erythrocytes at upstream microvessel area because of large distribution of "sphincter-like" structures in pial arteries but less distribution in intracerebral arterioles, capillaries, and veins[53,54].

In summary, I have shown dissociated responses between rCBF and rCBV during neuronal activation in the occipital cortex through simultaneous measurements using fMRI and NIOI. Cooperative measurements using these two techniques are expected to provide complementarily more detailed physiological interpretation of functional brain mappings.

ACKNOWLEDGEMENTS

I thank Dr. Junji Seki, Dr. Satoru Miyauchi, Dr. T. Kuroda-Tamada, and Dr. T. Hayakawa for helpful comments and suggestions, and Mr. Shigeyuki Kan (Doctor course student of Kyushu Institute of Technology Graduate School of Life Science and System Engineering) to support of measurement of FAIR-fMRI.

REFERENCES

1) Ogawa S, Lee TM, Kay AR, Tank DW: Brain magnetic resonance imaging with contrast dependent on blood oxygenation. Proc Natl Acad Sci USA, 1990; 87: 9868–9872
2) Ogawa S, Tank DW, Menon R, Ellermann JM, Kim S-G, Merkle H, Ugurbil K: Intrinsic signal changes accompanying sensory stimulation: functional brain mapping with magnetic resonance imaging. Proc Natl Acad Sci USA, 1992; 89: 5951–5955
3) Turner R (1992): Magnetic Resonance Imaging of Brain Function. Am J Physiol Imag, 1992; 314: 136–145
4) Moonen CT, Bandettini PA: Functional MRI. Berlin: Springer, 1999
5) Maki A, Yamashita Y, Ito Y, Watanabe E, Koizumi H: Spatial and temporal analysis of human motor activity using noninvasive NIR topography. Med Phys, 1995; 22: 1997–2005
6) Chance B, Anday E, Nioka S, Zhou S, Hong L, Worden K, Li C, Murray T, Ovetsky Y, Pidikiti D, Thomas R: A novel method for fast imaging of brain function, non-invasively, with light. Optics Express, 1998; 2: 411–423
7) Toronov V, Webb A, Choi JH, Wolf M, Michalos A, Gratton E, Hueber D: Investigation of human brain hemodynamics by simultaneous near-infrared spectroscopy and functional magnetic resonance imaging. Med Phys, 2001; 28: 521–527
8) Gratton G, Corballis PM, Cho E, Fabiani M, Hood DC: Shades of gray matter: noninvasive optical images of human brain responses during visual stimulation. Psychophysiol, 1995; 32: 505–509
9) Steinbrink J, Kohl M, Obrig H, Curio G, Syre F, Thomas F, Wabnitz H, Rinneberg H, Villringer A: Somatosensory evoked fast optical intensity changes detected non-invasively in the adult human head. Neurosci Lett, 2000; 291: 105–108
10) Adachi-Usami E: Human visual system modulation transfer function measured by evoked potentials. Neurosci Lett, 1981; 23: 43–47
11) Fox PT, Raichle ME: Stimulus rate dependence of regional cerebral blood flow in human striate cortex, demonstrated by positron emission tomography. J Neurophysiol, 1984; 51: 1109–1120
12) Vafaee MS, Meyer E, Marrett S, Paus T, Evans AC, Gjedde A: Frequency-dependent changes in cerebral metabolic rate of oxygen during activation of human visual cortex. J Cereb Blood Flow Metab, 1999; 19: 272–277
13) Kwong KK, Belliveau JW, Chesler DA, Goldberg IE, Weisskoff RM, Poncelet BP, Kennedy DN, Hoppel BE, Cohen MS, Turner R, Cheng H-M, Brady TJ, Rosen BR: Dynamic magnetic resonance imaging of human brain activity during primary sensory stimulation. Proc Natl Acad Sci USA, 1992; 89: 5675–5679
14) Thomas CG, Menon RS: Amplitude response and stimulus presentation frequency response of human primary visual cortex using BOLD EPI at 4 T. Magn Reson Med, 1998; 40: 203–209
15) Raichle ME: Circulatory and metabolic correlates of brain function in normal humans. In: Plum F, editor. Handbook of Physiology. The Nervous System V: Higher Functions of the Brain. Bethesda, MD: Am Physiol Soc, 1987: 643–674
16) Grubb RL, Raichle ME, Eichling JO, Ter-Pogossian MM: The effects of changes in $PaCO_2$ on cerebral blood volume, blood flow and vascular mean transit time. Stroke, 1974; 5: 630–639
17) Sase I, Eda H, Seiyama A, Tanabe HC, Takatsuki A, Yanagida T: Multi-channel optical mapping: Investigation of depth information. SPIE Biomed Optics, 2001; 4250: 29–36
18) Takatsuki A: Evaluation of spatio- and temporal-resolutions of near infrared spectroscopy for functional neural imaging of human subjects. Master's Thesis of Osaka University (in Japanese), 2002
19) Seiyama A, Seki J, Tanabe HC, Sase I, Takatsuki A, Miyauchi S, Eda H, Hayashi S, Imaruoka T, Iwakura T, Yanagida T: Circulatory basis of fMRI signals: relationship between changes in the hemodynamic

parameters and BOLD signal intensity. NeuroImage, 2004 ; 21 : 1204–1214
20) Keller E, Nadler A, Alkadhi H, Kollias SS, Yonekawa Y, Niederer P : Noninvasive measurement of regional cerebral blood flow and regional cerebral blood volume by near-infrared spectroscopy and indocynanine green dye dilution. NeuroImage, 2003 ; 20 : 828–839
21) Nelson SR, Manth ML, Maxwell JA : Use of specific gravity in the measurement of cerebral oedema. J Appl Physiol, 1971 ; 30 : 268–271
22) Lammertsma AA, Brooks DJ, Beaney RP, Turton DR, Kensett MJ, Heather JD, Marshall J, Jones T : In vivo measurement of regional cerebral haematocrit using positron emission tomography. J Cereb Blood Flow Metab, 1980 ; 4 : 317–322
23) Seiyama A, Hazeki O, Tamura M : Noninvasive quantitative analysis of blood oxygenation in rat skeletal muscle. J Biochem, 1988 ; 103 : 419–424
24) Hart WM Jr : The temporal responsiveness of vision. In : Hart WM Jr, editor. Adler's Physiology of the Eye. St. Louis : Mosby Year Book, 1992 : 572–573
25) Movshon JA, Thompson ID, Tolhurst DJ : Spatial and temporal contrast sensitivity of neurons in areas 17 and 18 of the cat's visual cortex. J Physiol, 1978 ; 283 : 101–120
26) Veringa F : Diffusion model of linear flicker responses. J Opt Soc Amer, 1970 ; 60 : 285–286
27) Kelly DH : Adaptation effects on spatio-temporal sine-wave thresholds. Vision Res, 1971 ; 12 : 89–101
28) Kelly DH : Motion and vision. II. Stabilized spatio-temporal threshold surface. J Opt Soc Amer, 1979 ; 69 : 1340–1349
29) Kaufmann C, Elbel G-K, Gossl C, Putz B, Auer DP : Frequency dependence and gender effects in visual cortical regions involved in temporal frequency dependent pattern processing. HHuman Brain Mapp, 2001 ; 14 : 28–38
30) Hagenbeek E, Rombouts SARB, van Dijk BW, Barkhof F : Determination of individual stimulus-response curve in the visual cortex. HHuman Brain Mapp, 2002 ; 17 : 244–250
31) Germon TJ, Kane NM, Manara AR, Nelson RJ : Near-infrared spectroscopy in adults : effects of extracranial ischemia and intracranial hypoxia on estimation of cerebral oxygenation. Br J Anaesth, 1994 ; 73 : 503–506
32) Quaresima V, Sacco S, Totaro R, Ferrari M : Noninvasive measurement of cerebral hemoglobin oxygenation saturation using two near infrared spectroscopy approaches. J Biomed Optics, 2000 ; 5 : 201–205
33) Kurihara K, Kikukawa A, Kobayashi A : Cerebral oxygenation monitor during head-up and -down tilt using near-infrared spatially resolved spectroscopy. Clin Physiol Funct Imag, 2003 ; 23 : 177–181
34) Choi J, Wolf M, Toronov V, Wolf U, Polzonetti C, Hueber D, Safonova LP, Gupta R, Michalos A, Mantulin W, Gratton E : Noninvasive determination of the optical properties of adult brain : near-infrared spectroscopy approach. J Biomed Optics, 2004 ; 9 : 221–229
35) Phelps ME, Huang SC, Hoffman E, Kuhl DE : Validation of topographic measurement of cerebral blood volume with C-11-labeled carboxyhemoglobin. J Nucl Med, 1979 ; 20 : 328–334
36) Grubb RL, Raichle ME, Higgins CS, Eichling JO : Measurement of regional cerebral blood volume by emission tomography. Ann Neurol, 1978 ; 4 : 322–328
37) Kuhl DE, Alavi A, Hoffman EJ, Phelps ME, Zimmerman RA, Obrist WD, Bruce DA, Greenberg JH, Uzzell B : Local cerebral blood volume in head-injured patients. J Neurosurg, 1980 ; 52 : 309–320
38) Fox PT, Raichle ME, Mintun MA, Dence C : Nonoxidative glucose consumption during focal physiologic neural activity. Science, 1988 ; 241 : 462–464
39) Ito H, Takahashi K, Hatazawa J, Kim SG, Kanno I : Changes in human regional cerebral blood flow and cerebral blood volume during visual stimulation measured by positron emission tomography. J Cereb Blood Flow Metab, 2001 ; 21 : 608–612
40) Kim S-G, Ugurbil K : Comparison of blood oxygenation and cerebral blood flow effects in fMRI : Estimation of relative oxygen consumption change. Magn Reson Med, 1997 ; 38 : 59–65
41) Villringer A, Planck J, Hock C, Schleinkofer L, Dirnagl U : Near infrared spectroscopy (NIRS) : a new tool to study hemodynamic changes during activation of brain function in human adults. Neurosci Lett, 1993 ; 154 : 101–104
42) Meek JH, Elwell CE, Khan MJ, Romaya J, Wyatt JS, Delpy DT, Zeki S : Regional changes in cerebral haemodynamics as a result of a visual stimulus measured by near infrared spectroscopy. Proc R Soc Lond B, 1995 ; 261 : 351–356
43) Zhu X-H, Kim S-G, Andersen P, Ogawa S, Ugurbil K, Chen W : Simultaneous oxygenation and perfusion imaging study of functional activity in primary visual cortex at different visual stimulation frequency : Quantitative correlation between BOLD and CBF changes. Magn Reson Med, 1998 ; 40 : 703–711
44) Logothetis NK, Pauls J, Augath M, Trinath T, Oeltermann A : Neurophysiological investigation of the basis of the fMRI signal. Nature, 2001 : 412 : 150–157
45) Hoge RD, Atkinson J, Gill B, Crelier GR, Marrett S, Pike B : Linear coupling between cerebral blood flow and oxygen consumption in activated human cortex. Proc Natl Acad Sci USA, 1999 ; 96 : 9403–9408
46) Buxton RB, Frank LR : A model for the coupling between cerebral blood flow and oxygen metabolism during neural stimulation. J Cerebr Blood Flow Metab, 1997 ; 17 : 64–72
47) Gjedde A, Poulsen PH, Ostergaard L : On the oxygenation of hemoglobin in the human brain. Adv Exp Med Biol, 1999 ; 471 : 67–81
48) Hyder F, Shulman RG, Rothman DL : A model for the regulation of cerebral oxygen delivery. J Appl Physiol, 1998 ; 85 : 554–564
49) Buxton RB : The elusive initial dip. NeuroImage, 2001 : 13 : 953–958
50) Roland PE, Eriksson L, Stone-Elander S, Widen L : Does mental activity change the oxidative metabolism of the brain ? J Neurosci, 1987 ; 7 : 2373–2389
51) Sakai F, Natazawa K, Tazaki Y, Ishii K, Hino H, Igarashi H, Kanda T : Regional cerebral blood volume and hematocrit measured in normal human volunteers by

single-photon emission computed tomography. J Cereb Blood Flow Metab, 1985 ; 5 : 207–213
52) Lu H, Golay X, Pekar JJ, Zijl PCM : Functional magnetic resonance imaging based on changes in vascular space occupancy. Magn Reson Med, 2003 : 50 : 263–274
53) Edvinsson L, Mackenzie ET, McCulloch J : Cerebral Blood Flow and Metabolism. New York : Raven Press, 1993
54) Lee RMKW : Morphology of cerebral arteries. Pharmac Ther, 1995 ; 66 : 149–173